SAND2020-5451C

EXPLORING EXPERIMENTAL PROCEDURES ON CRITICAL PARAMETERS FOR LOCALIZED CORROSION

R. M. Katona[1, 2] and R. G. Kelly[1]

[1] Materials Science and Engineering, University of Virginia, Charlottesville, VA 22904 USA
[2]Sandia National Laboratories, Albuquerque, NM 87123 USA

Key words: stainless steel, pitting corrosion, 1-D artificial pit

Abstract

Key factors leading to the determination of corrosion stability for stainless steel 304L (SS304L) are presented in a dilute sodium chloride solution. This evaluation was carried out by experimentally determining the pit stability product ($(i \cdot x)_{sf}$) and repassivation potential (E_{rp}) while varying the experimental scan rate. Overall, it was found that $(i \cdot x)_{sf}$ is independent of scan rate and E_{rp} is independent above a scan rate of 0.5 mV/sec. The overall influence of scan rate on led-in-pencil measurements will be discussed.

Introduction

Type 300 stainless steels (SS) are used heavily in marine environments due to their overall corrosion resistance.[1] Although characterized as a corrosion resistant alloy, SS's are susceptible to localized corrosion in the presence of an aggressive anion species, including chloride, the dominant anion in marine atmospheres. Localized corrosion, namely pitting corrosion, involves spatially localized metal oxidation creating metal cations in the pit cavity which result in aggressive chemistries due to hydrolysis reactions.[1] A critical condition for pit stability has been given as the need to exceed the pitting potential (E_{pit}). Stability for pitting corrosion has been described as the need for the potential exceed the repassivation potential (E_{rp}) and the current density (i) at a given pit depth (x) to exceed the pit stability product ($i \cdot x$).[2] Insights into pitting corrosion severity can be gained by comparing these phenomena[3].

Galvele originally showed that for a one-dimensional pit to sustain dissolution, the quantity $(i \cdot x)$ must exceed a critical value.[4] Stability is a battle between the production of acidity (via hydrolysis of metal cations produced by the dissolution current density) and diffusion of that concentrated solution to the bulk, which is controlled by the diffusion distance, x. Thus, a shallow pit requires a high current density to maintain stability, whereas a deep pit requires lower current density.

E_{pit} is dependent on experimental conditions as well as experimental technique causing a wide scatter in literature values.[2] However, assuming that a pit is actively growing on the surface, the growth phenomenon can be explained by transport phenomena and includes competitive adsorption, salt formation, film contamination among other phenomenon.[4] An original model developed by Pickering and Frankenthal,[5] exploited a one-dimensional pitting situation in which diffusion of metal cations from a pit was considered. However, this model could not be applied in its original form to all pitting cases because it would lead to an increase in pH in the pit as it grew. This model was improved by Galvele and a summary is provided below.[4]

As seen in Figure 1, Galvele used a geometry in which an active corroding metal was surrounded by a passive surface which was not undergoing corrosion.[4] That is, there is a flux (J) of metal ions from the metal surface at the bottom of the pit with no flux from the passive walls surrounding. When a metal undergoes anodic dissolution, a general expression for the anodic reaction taking place can be given by,

$$Me = Me^{n+} + ne^{-} \qquad (1)$$

where Me is the metal of interest, in this case SS304, and n is the number of electrons transferred during the anodic dissolution.[6] Based on stoichiometric dissolution of the alloy used in this study, $n_{304} = 2.2$.[7] The reaction given in Equation (1) is assumed to occur in a given aggressive sodium salt solution with a non-complexing anion.

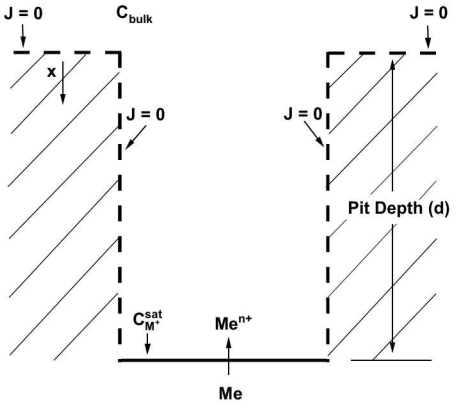

Figure 1: 1-Dimensional diffusion model exploited by Galvele formulism. It is pointed out in the original formulism that a saturation concentration was not required on the surface of the alloy for the original determination of the pit stability product and is further discussed in the introduction section. This figure is adapted from the original work of Galvele.[3]

Through the consideration of metal hydrolysis and mass transport in the 1-D scenario, the pit stability product is given by,

$$id = nFD_{M^+}\Delta C = (i \cdot x) \qquad (2)$$

It is noted that Galvele's original formulism did not include the presence of a salt film on the surface of the alloy which will be discussed in the subsequent paragraph. Thus, by considering the transport of ionic species in and out of the pit, the determination of the critical value $(i \cdot x)$ can be achieved. This pit stability product can be interpreted in the following way: if at a certain depth (x) the anodic dissolution current density (i) is insufficient to meet the pit stability criterion, the pit will repassivate because the critical chemistry will be lost to the bulk by diffusion. Experimentally this geometry can be exploited by a lead-in-pencil configuration. By mounting a thin wire in a non-conductive epoxy, the diffusion situation in Figure 1 can be created.

Galvele's original formulism only accounted for the diffusion of cations in solution and did not account for any complexation in the solution.[4] It was later found that pits propagating on the surface of an alloy can be under the presence of a metal salt film on the pit surface.[2] That is, when metal ions in solution reach a critical concentration, the metal ions combine with chloride anions in solution and precipitate, forming a dynamic metal-chloride salt complex on the surface of the dissolving alloy. This situation provides for a limiting current density i_{lim} of metal cations through the salt film and changes the formulism of Equation (2) to the following:

$$i_{lim}d = nFD_{M^+}C_{M^+}^{sat} = (i \cdot x)_{sf} \qquad (3)$$

where $C_{M^+}^{sat}$ is the saturation concentration of metal cations and the subscript sf denotes the presence of a salt film on the surface of the alloy.[2,7] This formulism will be exploited in experimentation. Along with this notation change, it is also noted that this critical value is for a 1-D geometry. The value of $(i \cdot x)_{sf}$ can be converted to a 3-D hemispherical geometry, which is more realistic of atmospheric

corrosion, and is based on the geometric flux from a corroding pit.[3]

Critical factors for localized corrosion have been typically explored at very few scan rates. However, a complete study of this has not been performed. Therefore, critical factors for localized corrosion will be explored at across various scan rates and the impacts on localized corrosion will be explored.

Experimental

Artificial pit set-up: $(i \cdot x)_{sf}$ and E_{rp} were determined for stainless steel 304L (SS304L) in dilute sodium chloride (0.6 M NaCl). Solutions were open to the atmosphere at ambient temperatures (25 $\pm$ 2 °C). The diameter of the SS304L wire was 50 µm. An example of this set up can be seen schematically in the work of Srinivasan et al.[8]. The epoxy and wire were wet ground with 320 grit silicon carbide paper. The wires were examined under an optical microscope in order to ensure a cross-section of the wire was fully exposed.

Electrochemical technique: Electrochemical techniques for this method have been detailed elsewhere[8]. One key factor that is present in the formulism used is the scan rate which is applied after the potentiostatic hold. This was varied in this experiment from 0.1 mV/sec to 50 mV/sec. The impacts of scan rate on $(i \cdot x)_{sf}$ and E_{RP} were explored.

Results and Discussion

Across the two orders of magnitude of scan rates that were investigated, there were two different behaviors observed during experimentation. At slow scan rates ($\leq$ 0.5 mV/sec) the behavior seen is represented by 0.1 mV/sec scan seen in Figure 2. The scan is characterized by diffusion limited growth through a salt film, from 0.45 V to roughly -0.1 V, at which point a plateau is reached. Upon further depression of the potential, a second limited current density region ($i_{lim,2}$) is attained, roughly around 1.4 x 10^{-4} A/cm^2. The potential then reaches a potential which is representative of an open circuit potential (OCP). This potential is dependent upon the depth of pit and becomes more noble with increasing pit depth. Finally, after the apparent OCP, the cathodic reduction reaction, hydrogen evolution, is seen.

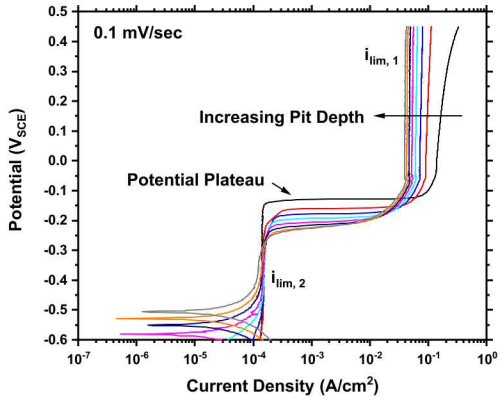

Figure 2: Artificial pit measurements on SS304L in 0.6 M NaCl performed at a scan rate of 0.1 mV/sec.

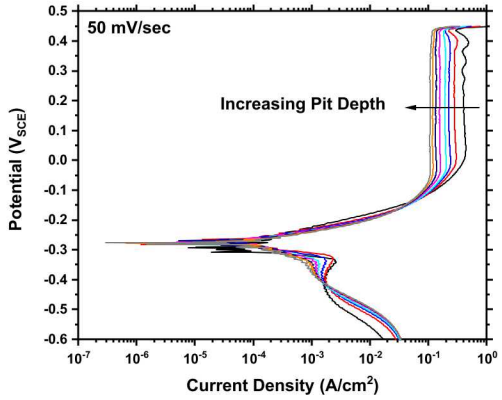

Figure 3: Artificial pit measurements on SS304L in 0.6 M NaCl performed at a scan rate of 50 mV/sec.

At faster scan rates (> 0.5 mV/sec), the behavior is representative of the 50 mV/sec scan seen in Figure 3. The scan is characterized by diffusion limited growth through a salt film from 0.45 V to roughly 0 V at which point an

activation/ohmic dissolution is reached. Upon further depression of the potential, the repassivation potential is reached [8]. Below E_{RP} the cathodic reduction reaction experiences a spike in current density around -0.35 V_{SCE} which is believed to be due to the deposition of copper on the surface of the alloy.

Although the behavior of the polarizations scans differs dependent on scan rate, $(i \cdot x)_{sf}$ is independent of scan speed with a reported value of 0.84 ± 0.03 A/m. $(i \cdot x)_{sf}$ was averaged from all scan rates between 0.1 mV/sec and 50 mV/sec with a corresponding error representing one standard deviation. This value is similar to those reported at a scan rate of 5 mV/sec in the same solution [9]. Another important factor ascertained from the lead-in-pencil tests performed in this experiment is E_{RP}. E_{RP} was evident[8] in fast scan rates (> 0.5 mV/sec) as shown in Figure 3. E_{RP} was found to be -0.27 ± 0.1 V_{SCE} and again was similar to previously reported values of at a scan rate of 5 mV/sec in the same solution [9].

As previously pointed out, at slow scan rates, a plateau in potential is reached between -0.1 and -0.3 $V_{SCE.}$ This potential decreases with increasing pit depth (Figure 2). During the potential plateau, the current density decreases rapidly and reaches a second limitation in current density (around 1.4 x 10^{-4} A/cm^2). This plateau in potential has been previously observed[10] however, does not match with presented theories of E_{RP} [8,11]. It is hypothesized that within this potential region, the scan rate is sufficiently slow to allow for dilution of metal cations out of the pit and the pit chemistry pH rises. When the potential is further scanned lower, a second limiting current density is reached and is believed to be the passivation current density. The passivation of SS304L has been explored in various solutions[12], however, the pH of the pit chemistry at this point is unknown and will likely influence the passivation current density. Further evidence is provided for significant dilution of metal cations as there is no current spike (-0.35 V_{SCE} Figure 3) which is representative of copper re-plating on the surface. This current peak is no longer seen as any copper from the dissolution reaction has diffused away from the surface. Although this is believed to be the case, the pH and chemistry of the surface is unknown. In order to confirm this hypothesis, modeling, in which species transport is considered, needs to be performed and is an area of interest.

Conclusions

Scan rate has shown to play a large roll on the behavior of lead-in-pencil measurements for SS304L in dilute NaCl. Pit stability product and repassivation potential were determined for dilute NaCl at various scan rates. Overall, $(i \cdot x)_{sf}$ is independent of scan rate while E_{RP} is independent of scan rate above 0.5 mV/sec. Below 0.5 mV/sec, significant dilution of the pit chemistry occurs and allows for passivation of the alloy surface. In order to confirm this hypothesis, enhanced information on the surface chemistry and determination of the governing factors of lead-in-pencil measurements are necessary and can be achieved through modeling.

Acknowledgements

Sandia National Laboratories is a multi-mission laboratory managed and operated by National Technology and Engineering Solutions of Sandia, LLC., a wholly owned subsidiary of Honeywell International, Inc., for the U.S. Department of Energy's National Nuclear Security Administration under contract DE-NA0003525. This document is SAND###.

References

1. McCafferty, E. *Introduction to Corrosion Science*. (2010).
2. Laycock, N. J. & Newman, R. C.

Localised dissolution kinetics, salt films and pitting potentials. *Corros. Sci.* **39**, 1771–1790 (1997).
3. Chen, Z. Y. & Kelly, R. G. Computational Modeling of Bounding Conditions for Pit Size on Stainless Steel in Atmospheric Environments. *J. Electrochem. Soc.* **157**, C69–C78 (2010).
4. Galvele, J. R. Transport Processes and the Mechanism of Pitting of Metals. *J. Electrochem. Soc.* **123**, 464–474 (1976).
5. Pickering, H. W. & Frankenthal, R. P. On the mechanisms of localized corrosion of iron and stainless steel I. Electrochemical Studies. *J. Electrochem. Soc.* **119**, 1297–1304 (1967).
6. Srinivasan, J., Liu, C. & Kelly, R. G. Geometric Evolution of Flux from a Corroding One-Dimensional Pit and Its Implications on the Evaluation of Kinetic Parameters for Pit Stability. *J. Electrochem. Soc.* **163**, C694–C703 (2016).
7. Woldemedhin, M. T., Srinivasan, J. & Kelly, R. G. Effects of environmental factors on key kinetic parameters relevant to pitting corrosion. *J. Solid State Electrochem.* **19**, 3449–3461 (2015).
8. Srinivasan, J., McGrath, M. J. & Kelly, R. G. A High-Throughput Artificial Pit Technique to Measure Kinetic Parameters for Pitting Stability. *J. Electrochem. Soc.* **162**, C725–C731 (2015).
9. Katona, R. M., Carpenter, J., Schindelholz, E. J. & Kelly, R. G. Prediction of Maximum Pit Sizes in Elevated Chloride Concentrations and Temperatures. *J. Electrochem. Soc.* **166**, C3364–C3375 (2019).
10. Li, T., Scully, J. R. & Frankel, G. S. Localized Corrosion: Passive Film Breakdown vs Pit Growth Stability: Part V. Validation of a New Framework for Pit Growth Stability Using One-Dimensional Artificial Pit Electrodes. *J. Electrochem. Soc.* **166**, C3341–C3354 (2019).
11. Anderko, A., Sridhar, N. & Dunn, D. S. A general model for the repassivation potential as a function of multiple aqueous solution species. *Corros. Sci.* **46**, 1583–1612 (2004).
12. Liu, C. & Kelly, R. G. Comparison study of the effect of oxide film properties on cathodic kinetics of stainless steel 304L and 316L during ORR potential window in sulfate solution. *Corrosion* **75**, 1087–1099 (2019).